EUROPEAN ORGANIZATION FOR NUCLEAR RESEARCH

CERN-PH-EP-2016-040
24 Novermer 2016

Systematic studies of correlations between different order flow harmonics in Pb–Pb collisions at $\sqrt{s_{\rm NN}} = 2.76$ TeV

ALICE Collaboration *

Abstract

The correlations between event-by-event fluctuations of amplitudes of anisotropic flow harmonics in Pb–Pb collisions at $\sqrt{s_{\rm NN}} = 2.76$ TeV were measured with the ALICE detector at the Large Hadron Collider. The results were obtained with the multi-particle cumulant method. The method is robust against systematic biases originating from non-flow effects. The centrality dependence of correlation between the higher Fourier harmonics (v_3, v_4, v_5) and the lower harmonics (v_2, v_3) as well as the transverse momentum dependence of v_3-v_2 and v_4-v_2 correlations are presented. ~~Comparisons are made~~ The results are compared to predictions from viscous hydrodynamics and A Multi-Phase Transport model (AMPT) models. The comparisons to viscous hydrodynamic models demonstrate that the different order Fourier harmonic correlations respond differently to the initial conditions or η/s and the small η/s regardless of initial conditions is flavored and the small η/s with the AMPT initial condition is closest to the results.

Together with the existing measurements of individual flow harmonics the presented results provide further constraints on initial conditions and the transport properties of the system produced in heavy-ion collisions.

*See Appendix **??** for the list of collaboration members

1 Introduction

The main emphasis of the ultra-relativistic heavy ion collisions at the Relativistic Heavy Ion Collider (RHIC) and the Large Hadron Collider (LHC) is to study deconfined phase of the strongly interacting matter, the Quark-Gluon Plasma (QGP). This matter exhibits strong collective and anisotropic flow in the transverse plane driven by the pressure gradients, with more particles emitted in the direction of the largest gradients. The large elliptic flow discovered at RHIC energies [**?**] continues to increase also in LHC energies [**? ?**]. This has been predicted by calculations utilising viscous hydrodynamics [**? ? ? ? ? ?**].

These calculations also demonstrated that the shear viscosity to the entropy density ratio (η/s) of strongly interacting matter is close to a universal lower bound $1/4\pi$ [**?**] in heavy ion collisions at RHIC and LHC energies.

The temperature dependence of the η/s has some generic features that most of the known fluids obey. One such general behavior is that the ratio typically reaches its minimum value close to the phase transition region [**?**]. It was shown, using kinetic theory and quantum mechanical considerations [**?**]~~that $\eta/s > 1/15$~~, that $\eta/s \sim 0.1$ would be an order of magnitude for the lowest possible shear viscosity to entropy ratio in nature. Later it was found that one can calculate an exact lower bound $(\eta/s)_{\rm min} = 1/4\pi \approx 0.08$ using the AdS/CFT correspondence [**?**]. Hydrodynamical simulations supports as well the view that the QGP matter indeed is close to that limit [**?**]. This in turn may have an important implications to other fundamental physics goals. It is argued that such a low value might imply that thermodynamic trajectories for the expanding matter would lie close to the QCD critical end point, which is another subject of intensive experimental quest [**?**].

Anisotropic flow is traditionally quantified with harmonics v_n and corresponding symmetry plane angles ψ_n in the Fourier series decomposition of particle azimuthal distribution in the plane transverse to the beam direction [**?**]:

$$E\frac{{\rm d}^3N}{{\rm d}p^3} = \frac{1}{2\pi}\frac{{\rm d}^2N}{p_{\rm T}{\rm d}p_{\rm T}{\rm d}\eta}\left\{1+2\sum_{n=1}^{\infty} v_n(p_{\rm T},\eta)\cos[n(\varphi-\Psi_n)]\right\}, \quad (1)$$

where E, N, p, $p_{\rm T}$, φ and η are the energy, particle yield, total momentum, transverse momentum, azimuthal angle and pseudorapidity of particles, respectively, and Ψ_n is the azimuthal angle of the symmetry plane of the $n^{\rm th}$-order harmonic. The $n^{\rm th}$-order flow coefficients are denoted as v_n and can be derived as $v_n = \langle\cos[n(\varphi-\Psi_n)]\rangle$, where the brackets denote an average over all particles in all events.

The anisotropic flow is understood as hydrodynamic response to spatial deformation of the initial density profile. This profile fluctuates ~~event to event due to quantum~~ event-by-event due to fluctuations of the positions of the constituents inside the colliding nuclei, which in turn implies that the flow also fluctuates [**? ?**]. The recognition of the importance of flow fluctuation has led to triangular flow and higher harmonics [**? ?**] as well as the correlations between different Fourier harmonics [**?**]. ~~As the result from ATLAS experiments, it shows that~~

The higher order harmonics are ~~sensitive to the~~ expected to be particularly sensitive to fluctuations in the initial conditions and to the η/s ~~[?]~~[**? ?**]. And the v_n distributions carry detailed information about the initial density profile [**? ?**].

However, difficulties on extracting the shear viscosity in heavy ion has been realized since it strongly depends on the specific choice of the initial conditions [**? ? ?**]. The viscous effects reduce the magnitude of the elliptic flow. Furthermore, the magnitude of η/s used in these calculations should be considered as an average over the temperature history of the expanding fireball as it is known that η/s of other fluids depends on temperature. In addition, part of the elliptic flow can also originate from the hadronic

phase [? ? ?]. Therefore, knowledge of both the temperature dependence and the relative contributions from the partonic and hadronic phases should be understood better to quantify η/s of the partonic fluid.

The higher harmonics ($n > 3$) are understood as superpositions of linear and nonlinear responses, through which they are correlated with lower-order harmonics [? ?]. When the harmonic order is large, the nonlinear response contribution in viscous hydrodynamics is dominant [? ?]. The magnitude of the viscous corrections as a function of ~~p_{T}~~ p_{T} for v_4 and v_5 ~~are~~ is sensitive to ansatz used for the viscous distribution function, δf, a ~~small~~ correction for the equilibrium distribution at hadronic freeze-out~~when QGP phase has become cool and dilute~~ [?]. Hence the studies of the higher order ($n > 3$) to lower order (v_2 or v_3) harmonic correlations and their ~~p_{T}~~ p_{T} dependence can help to understand the viscous correction to the momentum distribution at hadronic freeze-out which is probably the least understood part of hydrodynamic calculations [? ?].

Recently we measured for the first time the new multiparticle observables, the Symmetric 2-harmonic 4-particle Cumulants (SC), which quantify the relationship between event-by-event fluctuations of two different flow harmonics. The new observables are particularly robust against few-particle non-flow correlations and they provide orthogonal information to recently analysed symmetry plane correlators [?]. It was demonstrated that they are sensitive to the η/s of the expending medium and simultaneous descriptions of different order harmonic correlations would constrain both the initial conditions and the medium properties. In this article, we have extended the analysis to higher order Fourier harmonic (up to 5th order) correlations as well as ~~p_{T}~~ p_{T} dependence of correlations for the lower order harmonic (v_3-v_2 and v_4-v_2). We also include a systematic comparison to hydrodynamic and AMPT models. In Sec. ?? we present the details of the analysis methods. The experimental setting and measurements ~~is~~ are described in Sec. ?? and the sources of systematic uncertainties are explained in Sec. ??. The results of the measurements are presented in Sec. ??. In Sec. ?? we present comparisons to theoretical calculations. Sec. ?? summarizes our findings.

2 Theoretical models

We have used various models in this article. The HIJING model [? ?] was utilized to obtain the ~~p_{T}~~p_{T}-weights [?] which were used to estimate systematic bias due to non-uniform reconstruction efficiency. Secondly, the HIJING model was used to estimate the strength of non-flow correlations (typically few-particle correlations insensitive to the collision geometry).

We have compared the centrality dependence of our observables with theoretical model from [?], where the initial energy density profiles are calculated using a next-to-leading order perturbative-QCD+saturation model [? ?]. The subsequent spacetime evolution is described by relativistic dissipative fluid dynamics with different parametrizations for the temperature dependence of the shear viscosity to entropy density ratio $\eta/s(T)$. Each of the $\eta/s(T)$ parametrizations is adjusted to reproduce the measured v_n from central to mid-peripheral collisions.

The VISH2+1 [?] is an event-by-event theoretical framework model for relativistic heavy-ion collision based on (2+1)-dimensional viscous hydrodynamics which describes both the QGP fluid and the highly dissipative and even off-equilibrium late hadronic stage with fluid-dynamics. With well tuned transport coefficients, decoupling temperature and some well-chosen initial conditions (like AMPT [? ? ?] etc.), it could fit many related soft hadron data, such as the ~~p_{T}~~ p_{T} spectra and different flow harmonics at RHIC and the LHC [? ? ? ?]. Three different initial conditions (MC-Glauber, MC-KLN and AMPT) along with different constant η/s parametrizations are used in the model. Traditionally, the Glauber model constructs the initial entropy density of the QGP fireball from a mixture of the wounded nucleon and binary collision density profiles [?], and the KLN model assumes the initial entropy density is proportional to the initial gluon density calculated from the corresponding k_T factorization formula [?]. In the Monte-Carlo versions (MC-Glauber and MC-KLN) [? ? ?], additional initial state fluctuations are

introduced through the position fluctuations of individual nucleons inside the colliding nuclei. For the AMPT initial conditions [**?** **?** **?**], the fluctuating energy density profiles are constructed from the energy decompositions of individual partons, which fluctuate in both momentum and position space. Compared with the MC-Glauber and MC-KLN initial conditions, the additional Gaussian smearing parameter in the AMPT initial conditions makes the typical initial fluctuation scales changeable which gives rise to non-vanishing initial local flow velocities [**?**].

Finally, we provide an independent estimate of the centrality dependence of our observables by utilizing the AMPT model [**?** **?** **?**]. Even though thermalization could be achieved in collisions of very large nuclei and/or at extremely high energy, the dense matter created in heavy ion collisions may not reach full thermal or chemical equilibrium as a result of its finite volume and energy. To address such non-equilibrium many-body dynamics, AMPT has been developed, which includes both initial partonic and final hadronic interactions and the transition between these two phases of matter. For the initial conditions, the AMPT model uses the spatial and momentum distributions of hard minijet partons and soft strings from the HIJING model [**?** **?**]. The AMPT model can be run in two main configurations, the default and the string melting model. In the default version, partons are recombined with their parent strings when they stop interacting. The resulting strings are later converted into hadrons using the Lund string fragmentation model [**?** **?**]. In the string melting version, the initial strings are melted into partons whose interactions are described by the ZPC parton cascade model [**?**]. These partons are then combined into the final-state hadrons via a quark coalescence model. In both configurations, the dynamics of the subsequent hadronic matter is described by a hadronic cascade based on a Relativistic Transport (ART) model [**?**] which also includes resonance decays. The third version presented in this article is based on the string melting configuration, in which the hadronic rescattering phase is switched off to study its influence to the development of anisotropic flow. The input parameters used in both configurations are: $\alpha_s = 0.33$, a partonic cross-section of 1.5 mb, while the Lund string fragmentation parameters were set to $\alpha = 0.5$ and $b = 0.9$ GeV^{-2}. Even though the string melting version of AMPT [**?** **?**] reasonably reproduces particle yields, p_{T} spectra, and v_2 of low-p_{T} pions and kaons in central and mid-central Au–Au collisions at $\sqrt{s_{\mathrm{NN}}} = 200$ GeV and Pb–Pb collisions at $\sqrt{s_{\mathrm{NN}}} = 2760$ GeV [**?**], it was seen clearly in the recent study [**?**] that it fails to quantitatively reproduce the measurements. It turns out that the radial flow in AMPT is 25% lower than the measured value at the LHC, which indicates that the unrealistically low radial flow in AMPT is responsible for the quantitative disagreement. The detail configurations on AMPT settings used for this article and the comparisons of ~~p_{T}~~–p_{T} differential v_n for pions, kaons and protons to the data can be found in [**?**].

3 Results

The centrality dependence of SC(4,2) and SC(3,2) are presented in Fig. **??** as shadow bands which are the same as the published results [**?**]. Positive values of SC(4,2) are observed for all measured centralities. This suggests a positive correlation between the event-by-event fluctuations of v_2 and v_4. It also indicates that finding v_2 larger than average ($\langle v_2 \rangle$) in an event enhances the probability of finding v_4 larger than average ($\langle v_4 \rangle$) in that event. On the other hand, the negative results of SC(3,2) over all measured centralities show the anti-correlation between v_2 and v_3 flow harmonic magnitudes, which further implies that finding v_2 larger than average ($v_2 > \langle v_2 \rangle$) enhancing the probability of finding smaller v_3 than average ($v_3 < \langle v_3 \rangle$).

The centrality dependence of the higher order harmonic correlations (SC(4,3), SC(5,2) and SC(5,3)) are presented in Fig. **??** and compared to the lower order harmonic correlations (SC(4,2),SC(3,2)). The correlation between v_3 and v_4 is negative as similarly as v_3 and v_2 while the others are all positive. The higher order flow harmonic correlations (SC(4,3), SC(5,2) and SC(5,3)) are much smaller compared to the lower order harmonics (SC(3,2) and SC(4,2)). Especially SC(5,2) is 10 times smaller than SC(4,2) and SC(4,3) is about 20 times smaller that SC(3,2).

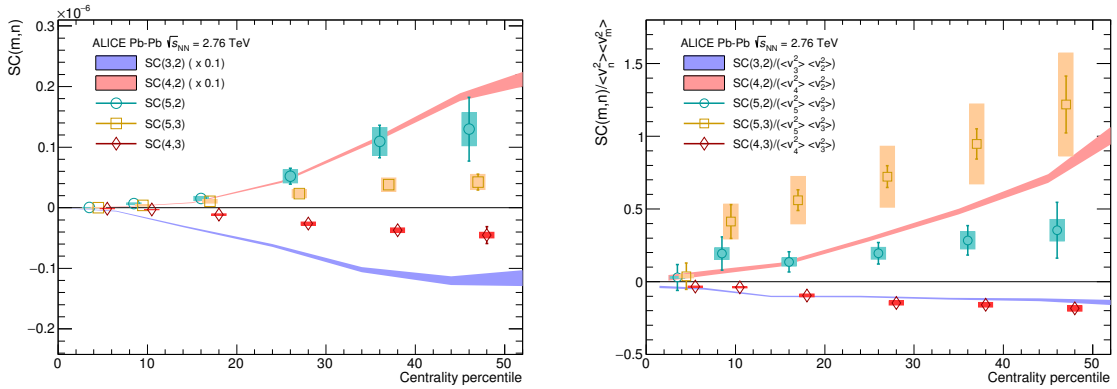

Fig. 1: The result of SC(m,n) (left figure) and NSC(m,n) (right figure) with flow harmonic order up to 5th in Pb–Pb $\sqrt{s_{\rm NN}} = 2.76$ TeV. Note that the lower order harmonic correlations (SC(4,2),SC(3,2)) are scaled down by factor of 10 and only statistical errors are shown in the left hand side figure.

However, unlike SC(m,n), NSC(m,n) results with the higher order flow harmonics show almost same order of the correlation strength as the lower order flow harmonic correlations (NSC(3,2) or NSC(4,2)). NSC(4,3)) is comparable to NSC(3,2) and one finds that a hierarchy NSC(5,3)>NSC(4,2)>NSC(5,2) holds for most of centrality ranges within the errors. These results indicate that the lower order harmonic correlations (SC(3,2) and SC(4,2)) are larger than higher order harmonic correlations (SC(4,3), SC(5,2) and SC(5,3)), not only because of the correlation strength itself but also the individual flow strength. SC(5,2) is stronger than SC(5,3), but as for NSC, the correlation between v_5 and v_3 is stronger than the correlation between v_5 and v_2.

To obtain the ~~p_T~~ $p_{\rm T}$ dependence of SC(m,n) results, we apply minimum ~~p_T~~ $p_{\rm T}$ cuts, instead of ~~p_T~~ $p_{\rm T}$ bin-by-bin interval in order to avoid large statistical fluctuations in the results. The various minimum ~~p_T~~ $p_{\rm T}$ cuts from 0.2 to 1.5 are applied. The results of ~~p_T~~ $p_{\rm T}$ dependence with SC(3,2) and SC(4,2) for minimum ~~p_T cuts, $0.2 < p_T < 0.7$~~ $p_{\rm T}$ cuts, $0.2 < p_{\rm T} < 0.7$, are shown on the left top in Fig. **??**. The strength of SC(m,n) correlation becomes larger as the minimum ~~p_T~~ $p_{\rm T}$ increases. This indicates that the relationship between event-by-event fluctuation of two different flow harmonics v_m and v_n is stronger for high ~~p_T~~ $p_{\rm T}$ particles. This ~~p_T~~ $p_{\rm T}$ dependence correlations have much stronger centrality dependence, where SC(m,n) gets much larger as the centrality or ~~p_T~~ $p_{\rm T}$ increase. NSC(3,2) and NSC(4,2) with different minimum cuts are shown on the right in Fig. **??**. The strong ~~p_T~~ $p_{\rm T}$ dependence observed in SC(m,n) is not clearly seen in NSC(m,n). NSC(m,n) results are aligned all together and consistent in errors for all minimum ~~p_T~~ $p_{\rm T}$ cuts. This suggests that the ~~p_T~~ $p_{\rm T}$ dependence of SC(m,n) does not solely result from the correlation between flow harmonics but results from the different values of ~~p_T~~ $p_{\rm T}$ dependent individual v_n values. The minimum ~~p_T~~ $p_{\rm T}$ cuts are extended from 0.8 to 1.5 ~~GeV/c~~ GeV/c and the results are shown on the bottom in Fig~~.~~ **??**. As for SC(m,n), the similar trends are observed as similarly as ~~$p_T < 0.8$~~ $p_{\rm T} < 0.8$, however NSC(m,n) tends to decrease as the minimum ~~p_T~~ $p_{\rm T}$ or the centrality increase. The ~~p_T~~ $p_{\rm T}$ dependence for NSC(3,2) is not clearly seen and it is consistent with no ~~p_T~~ $p_{\rm T}$ dependence within the current statistical and systematic errors except for 40-50% centrality and NSC(4,2) shows a moderate decreasing trend for increasing ~~p_T~~ $p_{\rm T}$ (see further discussions in Sec. **??**). This might be an indication of possible viscous corrections for the equilibrium distribution at hadronic freeze-out [**?**].

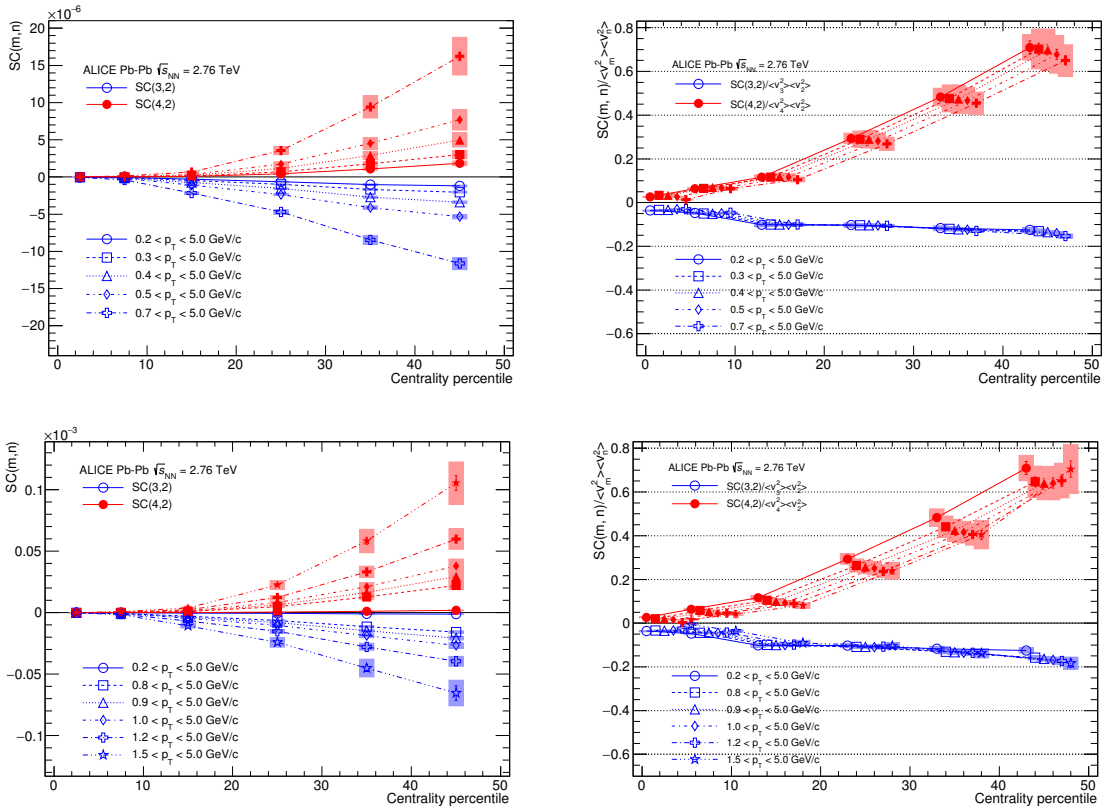

Fig. 2: SC(3,2) and SC(4,2) with various minimum ~~p_T~~ p_{T} cuts (~~Left~~left) and results of normalized SC(3,2) and SC(4,2) (~~Right~~right). The upper panels show the results for minimum ~~p_T~~ p_{T} range, ~~$0.2 < p_T < 0.7$ GeV/c~~ $0.2 < p_{\mathrm{T}} < 0.7$ GeV/c and the bottom panels are for minimum ~~p_T~~ p_{T} range, ~~$0.8 < p_T < 1.5$ GeV/c~~$0.8 < p_{\mathrm{T}} < 1.5$ GeV/c. Note that NSC data points from each minimum p_{T} in a centrality percentile bin are shifted for visibility.

4 Model comparisons

4.1 Low order harmonic correlations

SC(3,2) and SC(4,2) are compared to several theoretical calculations. First, the fluid hydrodynamic predictions with the different parameterizations for the temperature dependence of the shear viscosity to entropy ratio $\eta/s(T)$ are shown on the left in Fig. **??**. ~~Roughly the hydrodynamic calculations~~ The hydrodynamic calculations roughly capture qualitatively the centrality dependence, but not quantitively. Both SC(3,2) with data and hydrodynamics have negative values for all centralities, while SC(4,2) results have positive values over all measured centralities. However, there is no single centrality for which a given $\eta/s(T)$ parameterization describes both SC(3,2) and SC(4,2) simultaneously. On the other hand, the same hydrodynamic calculations capture the centrality dependence of the individual v_n quantitively [**?**].

NSC(3,2) and NSC(4,2) are also compared to the same model on the right in Fig. **??**. While NSC(3,2) ~~doesn't~~ does not show sensitivity to different $\eta/s(T)$ parameterizations, NSC(4,2) exhibit much better sensitivity than NSC(3,2) observable and the individual flow harmonics [**?**]. These findings indicate that NSC(3,2) observable is sensitive mainly to the initial conditions, while NSC(4,2) observable is sensitive to both the initial conditions and the system properties, which is consistent with the prediction from [**?**]. However, the sign of NSC(3,2) is positive in the models in 0-10% central collisions while it is negative in data. In the most central collisions the anisotropies originate mainly from fluctuations, i.e. the initial ellipsoidal geometry characteristic for mid-central collisions plays little role in this regime. Hence this observation will help to understand the fluctuations in initial conditions better. NSC(4,2) observable shows better sensitivity for different $\eta/s(T)$ parameterizations, i.e. medium property but the model cannot describe the centrality dependence nor the absolute values. These observed distinct discrepancies between data and models might indicate that the current understanding of initial conditions used in the model need to be revisited to further constrain the $\eta/s(T)$, considering the difficulties on separating the role of the η/s from the initial condition to the final state particle anisotropies [**?** **?**]. Hence the use of SC(m,n) and NSC(m,n) can provide new constraints on the detailed modeling of the initial-state condition and the fluctuations of the medium created in heavy ion collisions and the better constraints on the initial-state conditions will certainly improve the uncertainties of determining $\eta/s(T)$.

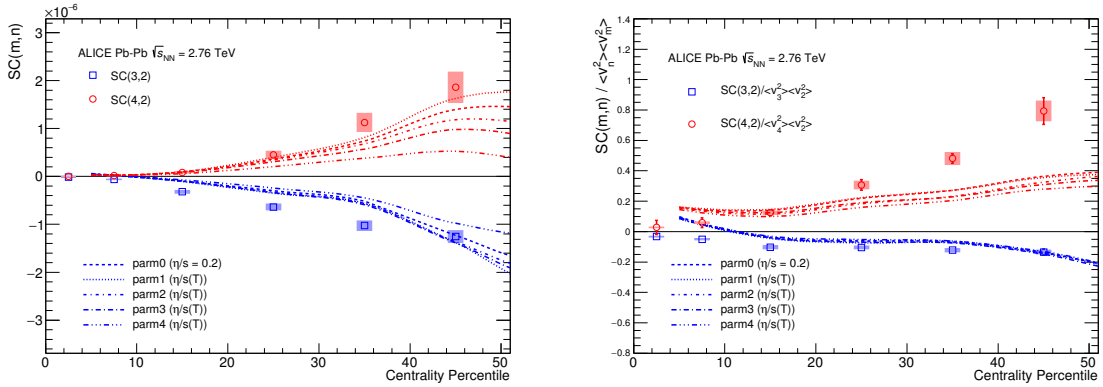

Fig. 3: Results from SC(m,n) in Pb–Pb $\sqrt{s_{\rm NN}} = 2.76$ TeV are compared to hydrodynamic calculations. The dashed lines are hydrodynamic predictions with various $\eta/s(T)$ parametrizations [**?**].

The results with the comparison to VISH2+1 calculation are shown in Fig. **??**. All the models with the large share viscosity regardless of the initial conditions (~~η/s=0.2~~ $\eta/s = 0.2$ for MC-KLN and MC-Glauber initial conditions and ~~$\eta/s = 0.16$~~ $\eta/s = 0.16$ for AMPT initial condition) ~~failed~~ fails to capture the centrality dependence of SC(3,2) and SC(4,2). And among the models with small shear viscosi-

ties (~~η/s=0.08~~$\eta/s = 0.08$), the one with the AMPT initial condition describes the data better both for SC(3,2) and SC(4,2) but they cannot describe the data quantitively for most of the centrality ranges. As similarly as the above mentioned hydrodynamic calculations [**?**], the sign of the normalised NSC(3,2) in these models is opposite to the data in 0-10% central collisions. NSC(3,2) ~~doesn't~~ does not show sensitivity to initial conditions or η/s parametrizations and cannot be described by these models quantitively. However, for NSC(4,2), it is sensitive both to initial conditions and η/s parametrizations. Even though NSC(4,2) is favoured both by AMPT initial condition with η/s=0.08 and MC-Glauber initial condition with ~~η/s=0.20~~$\eta/s = 0.20$, SC(4,2) can be only described by smaller η/s from AMPT and MC-Glauber initial conditions. Therefore the Glauber initial condition with ~~η/s=0.20~~ $\eta/s = 0.20$ model can be ruled out and we come to a conclusion based on the tested model parameters that η/s should be small and AMPT initial condition is favoured by the data.

Finally, the extracted results from particle level AMPT simulations in the same way as for the data are compared to the data in Fig. **??**. As for SC(3,2), neither of the settings can describe the data and the setting with the default AMPT model somewhat follows the trend of the data closest. The same setting can describe NSC(3,2) fairly well and also the sign of NSC(3,2) is well reproduced by this setting while all the hydrodynamic calculations in this article failed to describe the sign of the observable in the most central collisions. Interestingly the string melting AMPT model ~~can't~~ cannot capture the data well where the strength of the correlation is weaker than the default model. The third version based on the string melting configuration with the hadronic rescattering phase off is also shown to quantify its influence. This late hadronic rescattering stage makes both SC(3,2) and NSC(3,2) stronger in the string melting AMPT model but it is not enough to describe the data. Further we investigated why the default AMPT model can describe NSC(3,2) fairly well but underestimates SC(3,2). By taking the differences in the individual flow harmonics (v_2 and v_3) between the model and data into account, we were able to recover the ~~data~~difference in SC(3,2) between the data and the model. The discrepancy in SC(3,2) can be explained by the overestimated individual v_n values reported in [**?**] in all the centrality ranges.

In the case of SC(4,2), the string melting AMPT model can fairly well describe the data while the default model underestimates it. NSC(4,2) is slightly overestimated by the same setting which can describe SC(4,2) but the default AMPT model can describe the data better. The influence of the hadronic rescattering phase for NSC(4,2) is opposite to other observables (SC(3,2), NSC(3,2) and SC(4,2)), where the hadronic rescattering make NSC(4,2) slightly smaller. It should be noted that the better agreement for SC(m,n) should not be overemphasized since there are discrepancies in the individual v_n between AMPT and data as it was demonstrated for SC(3,2). Hence the simultaneous description of SC(m,n) and NSC(m,n) should give better constraints to the parameters in AMPT.

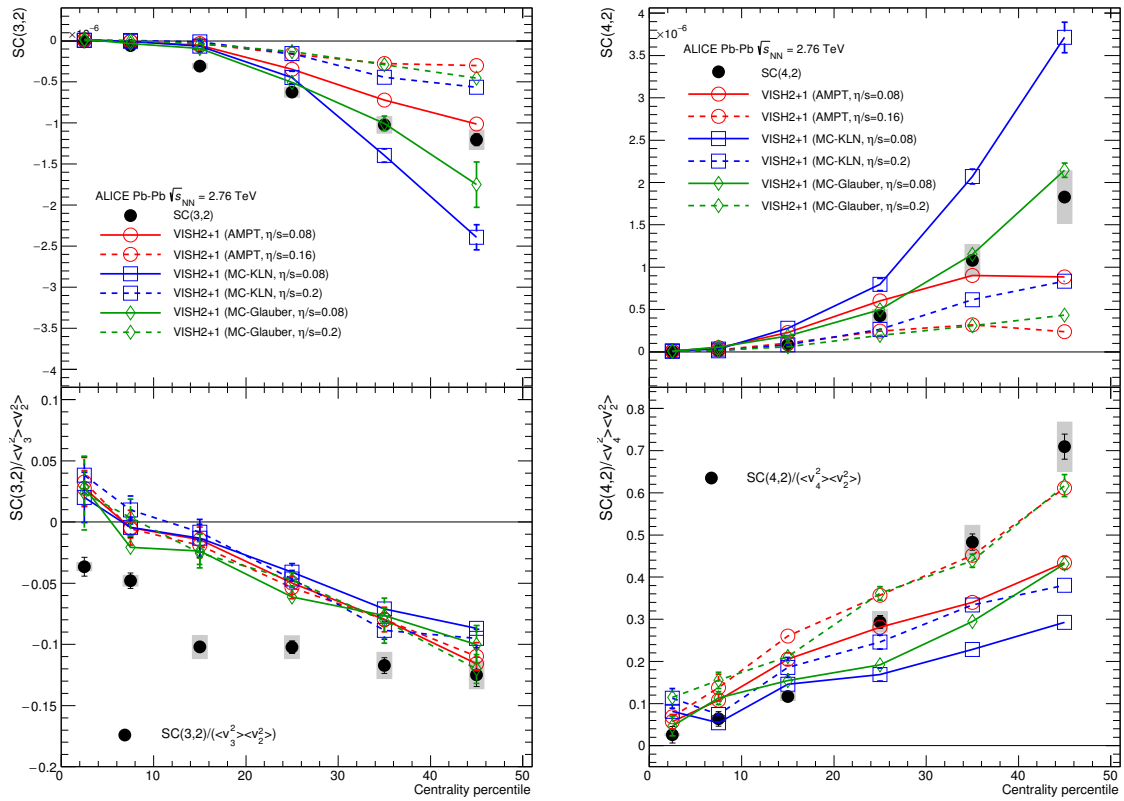

Fig. 4: Results of SC(3,2) and SC(4,2) are compared to various VISH2+1 calculations with different settings. Three initial conditions from AMPT, MC-KLN, and MC-Glauber are drawn as different colors and markers. The η/s parameters are shown as different line styles, the small shear viscosities (~~η/s=0.08~~$\eta/s = 0.08$) are shown as solid lines, and large shear viscosities (~~η/s=0.2~~ $\eta/s = 0.2$ for MC-KLN and MC-Glauber, 0.16 for AMPT) are drawn as dashed lines. Upper panels are the result of SC(m,n) and lower panels are the results of NSC(m,n).

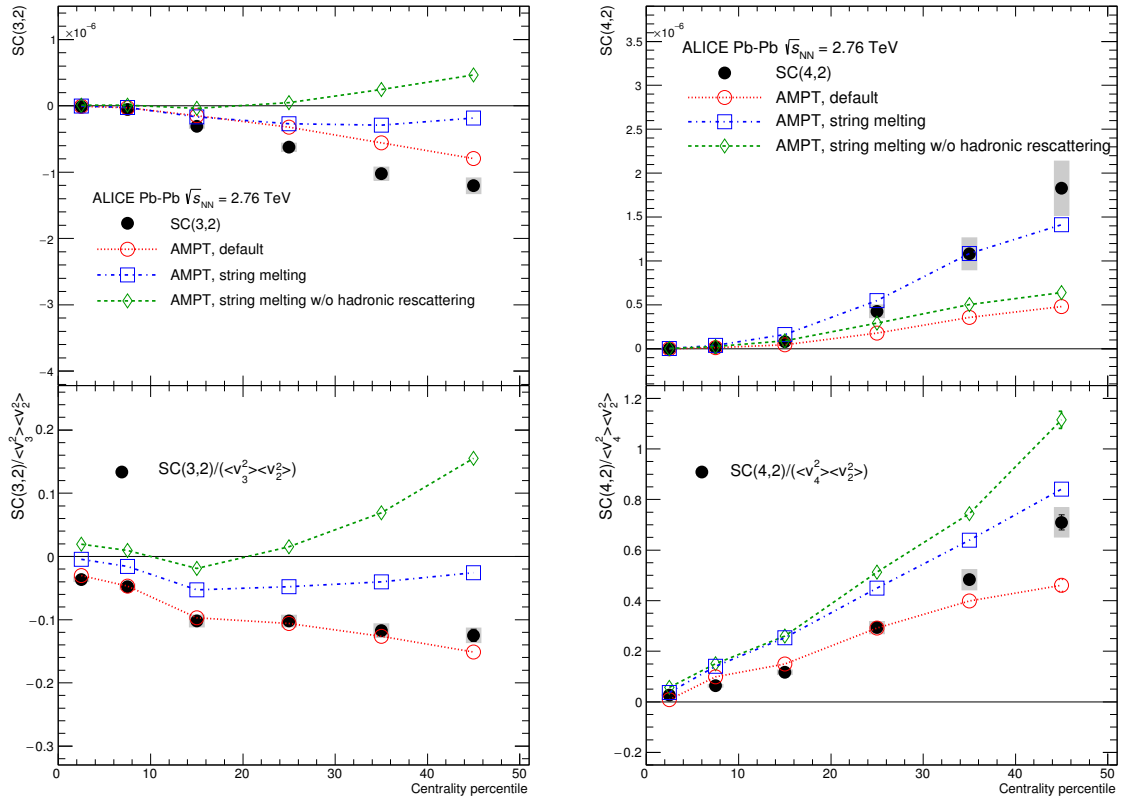

Fig. 5: Results of SC(3,2) and SC(4,2) are compared to various AMPT simulations. Upper panels are the results of SC(m,n) and the lower panels are the results of NSC(m,n). The details of the AMPT configurations can be found in Sec. **??**.

4.2 Higher order harmonic correlations

The higher order harmonic correlations (SC(4,3), SC(5,2) and SC(5,3)) are compared to VISH2+1 calculation, shown in Fig. **??**. All the models with the large share viscosity regardless of the initial conditions (~~η/s=0.2~~ $\eta/s = 0.2$ for MC-KLN and MC-Glauber initial conditions, and ~~$\eta/s = 0.16$~~ $\eta/s = 0.16$ for AMPT) failed to capture the centrality dependence of SC(5,2), SC(5,2) and SC(5,3), more clearly than lower order harmonic correlations (SC(3,2), SC(4,2)). And among the models with small shear viscosity (~~η/s=0.08~~$\eta/s = 0.08$), the one from the AMPT initial condition describes the data much better than the other initial conditions. A quite clear separation between different initial conditions is observed for these higher order harmonics correlations compared to the lower order harmonic correlations. NSC(5,2) and SC(5,3) are quite sensitive to both the initial conditions and the η/s parametrizations. As similarly as the above mentioned hydrodynamic calculations [**?**], the sign of the normalised NSC(4,3) in these models is opposite to the data in 0-10% central collisions. NSC(4,3) shows sensitivity to both initial conditions and η/s parametrizations while NSC(3,2) didn't show sensitivity to initial conditions or η/s parametrizations. SC(4,3) data is clearly favoured by smaller η/s but NSC(4,3) cannot be described by these models quantitively.

The extracted results from particle level AMPT simulations in the same way as for the data are compared to the data in Fig. **??**. The string melting AMPT model describes SC(5,2) and SC(5,3) well. The same setting describes only NSC(5,3) but it overestimates NSC(5,2). However the default AMPT model can describe NSC(5,3) and NSC(5,2) fairly well as similarly as NSC(3,2) and NSC(4,2).

in the case of SC(4,3), neither of the settings can describe the data but the default AMPT model follows the data closest. The string melting AMPT model fails to describe SC(4,3) and NSC(4,3). In summary, the default AMPT model describes the normalized SC (NSC(m,n)) from lower to higher order harmonic correlation while the string melting AMPT model overestimates NSC(5,2) and underestimates (or very weak correlations) NSC(4,3).

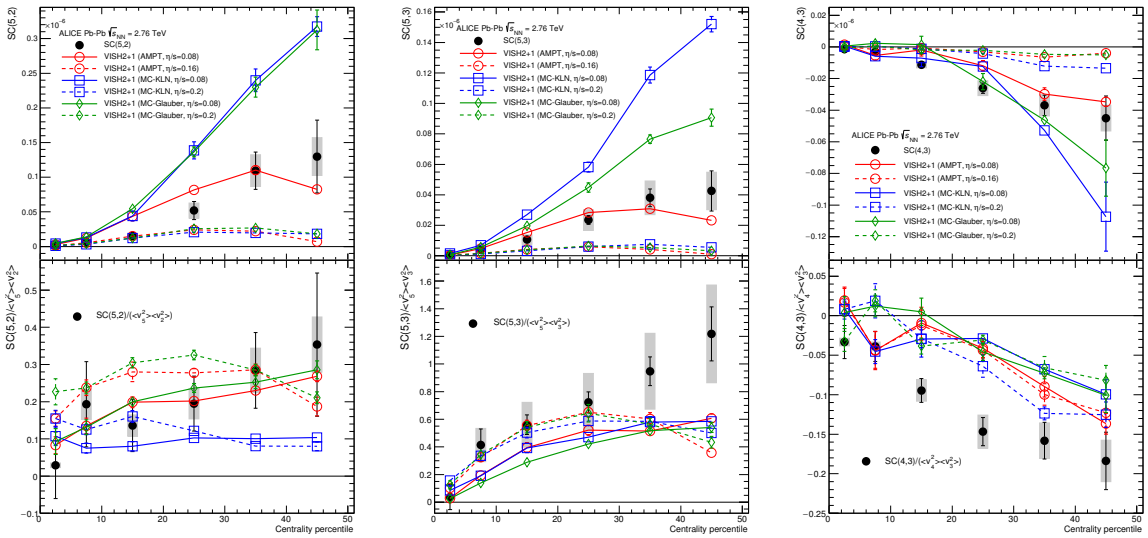

Fig. 6: Results of SC(5,2), SC(5,3) and SC(4,3) are compared to various VISH2+1 calculations. Three initial conditions from AMPT, MC-KLN and MC-Glauber are drawn as different colors and markers. The η/s parameters are shown as different line styles, the small shear viscosity (~~η/s=0.08~~$\eta/s = 0.08$) are shown as solid lines, and large shear viscosities (~~η/s=0.2~~ $\eta/s = 0.2$ for MC-KLN and MC-Glauber, 0.16 for AMPT) are drawn as dashed lines. Upper panels are the results of SC(m,n) and lower panels are the results of NSC(m,n).

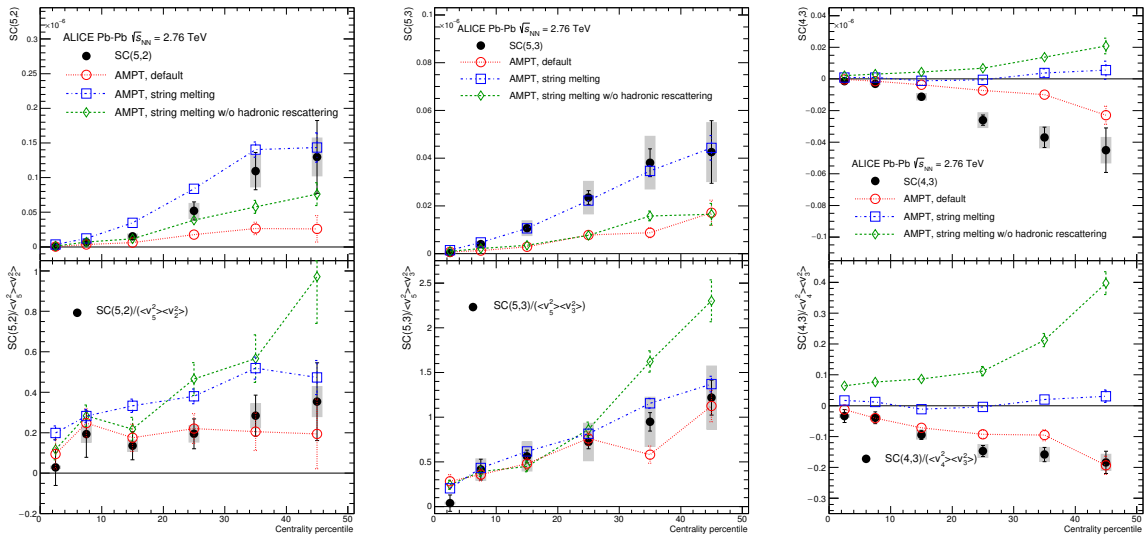

Fig. 7: Results of SC(5,2), SC(5,3) and SC(4,3) are compared to various AMPT simulations. Upper panels are the results of SC(m,n) and the lower panels are the results of NSC(m,n). The details of the AMPT configurations can be found in Sec. **??**.

4.3 Transverse momentum dependence of Low order harmonic correlations

NSC(3,2) and NSC(4,2) as a function of different minimum ~~p_T~~ p_{T} cut are compared to the AMPT simulations in Fig. **??**. As discussed in Sec. **??**~~in higher minimum p_T cuts, the p_T ,~~ the p_{T} dependence for NSC(3,2) and NSC(4,2) in mid central collisions is seen also in AMPT simulations for higher minimum p_{T} cuts. The other AMPT configurations except for the default AMPT model give very strong ~~p_T~~ p_{T} dependence above 1 ~~GeV/c~~ GeV/c and cannot describe the magnitude of the data both for NSC(3,2) and NSC(4,2). In the case of NSC(3,2), the default AMPT model describes the magnitude and ~~p_T~~ p_{T} dependence well in all collision centralities except for $40-50\%$ where the model underestimates the data and have stronger ~~p_T~~ p_{T} dependence than the data. As for NSC(4,2), the same model which describes NSC(3,2) also can reproduce the data well expect for $10-20\%$ and $40-50\%$ centralities where some deviations from the data both for the magnitude and ~~p_T~~ p_{T} dependence are observed. When the string melting AMPT model is compared to the same model with the hadronic rescattering off, it is observed that the very strong ~~p_T~~ p_{T} dependence as well as the correlation strength get weaker by the hadronic rescattering. This might imply that the hadronic interaction is the source of this observed ~~p_T~~ p_{T} dependence even though the relative contributions from partonic and hadronic stage in the final state particle should be studied further. This observed moderate ~~p_T~~ p_{T} dependence in mid central collisions both for NSC(3,2) and NSC(4,2) might be an indication of possible viscous corrections for the equilibrium distribution at hadronic freeze-out predicted in [**?**]~~when QGP phase has become cool and dilute~~.

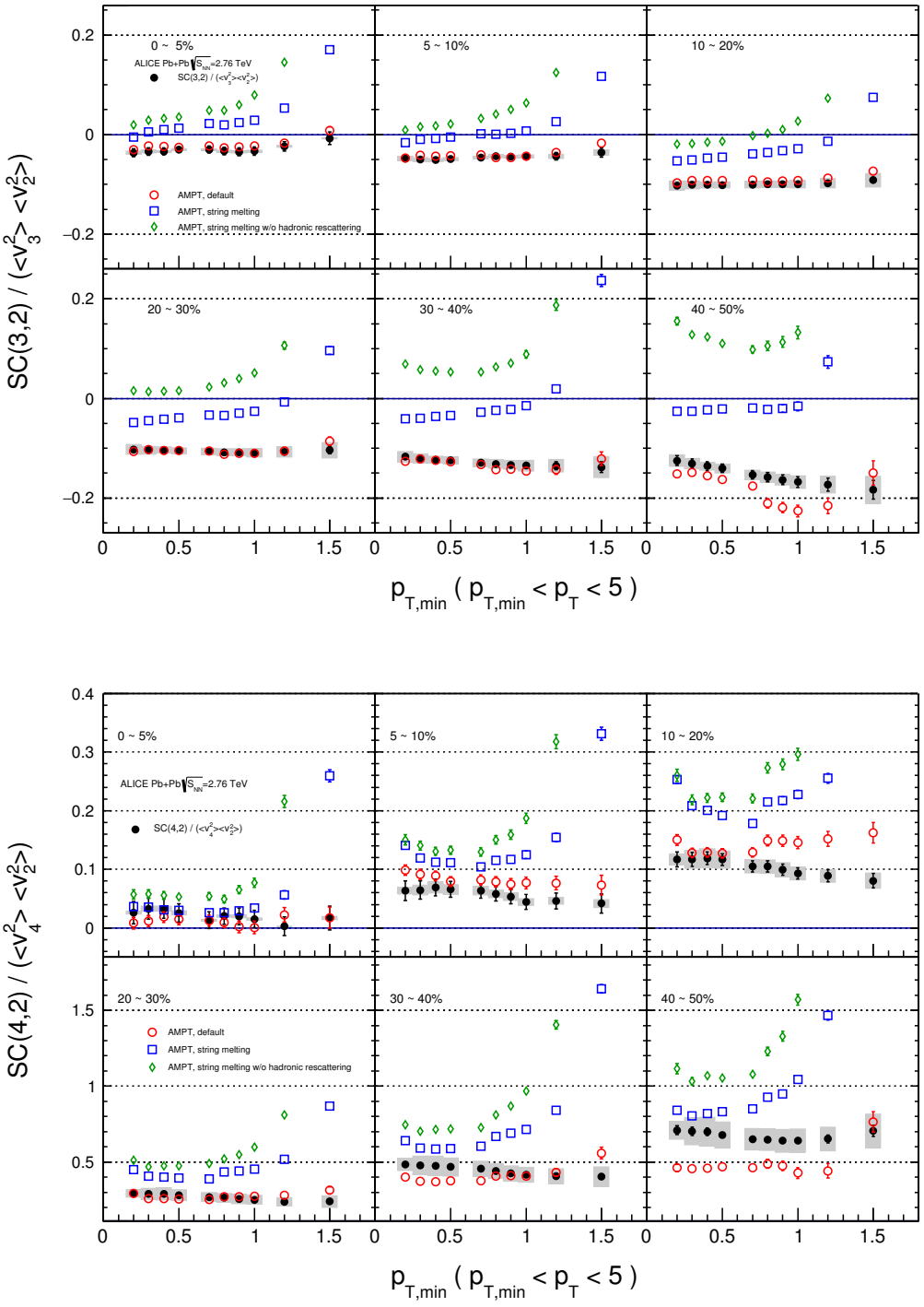

Fig. 8: NSC(3,2) (Top) and SC(4,2) (Bottom) as a function of minimum ~~p_T~~ p_{T} cuts. The AMPT results are drawn as color bands for comparison. The details of the AMPT configurations can be found in Sec. **??**.

5 Summary

In summary, we have measured the Symmetric 2-harmonic 4-particle Cumulants (SC), which quantify the relationship between event-by-event fluctuations of two different flow harmonics. The observables are particularly robust against few-particle non-flow correlations and they provide orthogonal information to recently analysed symmetry plane correlators. We have found that fluctuations of v_2 and v_3 (v_3 and v_4) are anti-correlated in all centralities and fluctuations of v_2 and v_4 (v_2 and v_5, v_3 and v_5) are correlated for all centralities. This feature was explored to discriminate between various hydro model calculations with different initial conditions as well as different parametrizations of the temperature dependence of η/s. We have found that the different order harmonic correlations have different sensitivities to the initial conditions and the system properties. Therefore they have discriminating power on separating the role of the η/s from the initial condition to the final state particle anisotropies. Furthermore, the sign of v_3-v_2 correlation in the model in 0-10% central collisions was found to be different between the data and hydrodynamic model calculations. In the most central collisions the anisotropies originate mainly from fluctuations, i.e. the initial ellipsoidal geometry characteristic for mid-central collisions plays little role in this regime. Hence this observation might help to understand the details of the fluctuations in initial conditions. The comparisons to VISH2+1 calculation show that all the models with the large share viscosity regardless of the initial conditions failed to capture the centrality dependence of higher order correlations, more clearly than lower order harmonic correlations and based on the tested model parameters that the η/s should be small and AMPT initial condition is flavored by the data. A quite clear separation of the correlation strength between different initial conditions is observed for these higher order harmonic correlations compared to the lower order harmonic correlations. Finally we have found that v_3-v_2 and v_4-v_2 correlations have moderate p_{T}-p_{T} dependence in mid central collisions. This might be an indication of possible viscous corrections for the equilibrium distribution at hadronic freeze-out. The results presented in this article can be used to further optimize model parameters and put better constraints on the initial conditions and the transport properties in ultra-relativistic heavy-ion collisions.

Acknowledgements

A The ALICE Collaboration